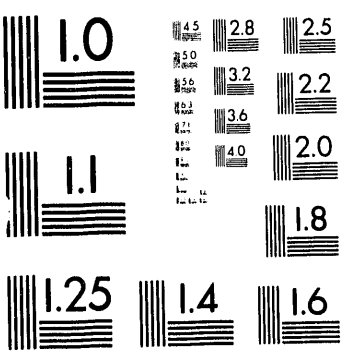
1.0
1.1
1.25
1.4
1.6
1.8
2.0
2.2
2.5
2.8
3.2
3.6
4.0
4.5
5.0
5.6

1 of 1

Distribution
Category UC-706

SAND93-1351
Unlimited Release
Printed August 1993

PROJECTILE TRANSVERSE MOTION AND STABILITY IN ELECTROMAGNETIC INDUCTION LAUNCHERS

I. R. Shokair
Sandia National Laboratories
Beam, Plasma, and Electromagnetic Theory Department
P. O. Box 5800
Albuquerque, New Mexico 87185

Abstract

The transverse motion of a projectile in an electromagnetic induction launcher is considered. The equations of motion for translation and rotation are derived assuming a rigid projectile and a flyway restoring force per unit length that is proportional to the local displacement. Transverse forces and torques due to energized coils are derived for displaced or tilted projectile elements based on a first order perturbation method. The resulting equations of motion for a rigid projectile composed of multiple elements in a multi-coil launcher are analyzed as a coupled oscillator system of equations and a simple stability condition is derived. The equations of motion are incorporated into the 2-D Slingshot code and numerical solutions for the transverse motion are obtained. For the 20 meter navy launcher parameters we find that stability is achieved with a flyway spring constant of $k \approx 1x10^8$ N/m^2. For $k = 1.5x10^8$ N/m^2 and sample coil misalignment modeled as a sine wave of 1 mm amplitude at wavelengths of one or two meters, the projectile displacement grows to a maximum of 4 mm. This growth is due to resonance between the natural frequency of the projectile transverse motion and the coil displacement wavelength. This resonance does not persist because of the changing axial velocity. Random coil displacement is also found to cause roughly the same projectile displacement. For the maximum displacement a rough estimate of the transverse pressure is 50 bars.

I. Introduction

The electromagnetic induction launcher accelerates a conducting armature by inducing armature currents opposite to the coil current, which result in a repulsive axial force that accelerates the armature.[1-2] Because of the finite resistivity the armature current decays and the magnetic field diffuses into the armature. For a solid armature, if the firing position of the coils is advanced (slipped) to account for field diffusion, near constant axial acceleration can be maintained.[3] For a wound armature,[4] no slipping is needed, but there is still field diffusion due to the finite resistivity resulting in an L/R decay of the acceleration. Because of the favorable distribution of current density in a wound aramature, voltage reversal can be used to significantly improve performance.

Although the acceleration is only in the axial direction, there are very large radial forces that act on both projectile and coils. Slight mis-alignments of coils can result in net transverse forces and torques on the projectile resulting in transverse motion. It is very important to insure that this motion is stable and to estimate the maximum amplitudes and induced stresses that result. This is the subject of this work. In section II we derive the equations of motion for both translation and rotation assuming a rigid projectile. It is assumed that the flyway tube restoring forces per unit length are proportional to the local displacement. In sections III and IV we derive the electromagnetic forces and torques that result when a projectile element is displaced or tilted from the axis of a coil, based on a first order perturbation method. In section V we write the equations of motion, for a multiple element projectile in a real launcher with many coils, in the form of coupled oscillators and consider the question of stability. Implementation of the transverse motion calculation in the Slingshot code[5] is then described in section VI. We also show numerical results of transverse motion using the modified Slingshot for the 20 meter navy gun parameters for a solid armature. Finally in section VII, the results are summarized. Presently we are working on an implementation of transverse motion in Slingshot for a wound armature and also are considering the effects of more accurate flyway tube restoring forces. Since the physical restoring forces in a launcher are functions of the axial position, it is expected that transverse motion will be significantly affected by this dependence.

II. Transverse Equations of Motion

In the one dimensional case the projectile transverse motion can be described by two variables x_0, the displacement of the projectile center of mass and θ, the angle of rotation of the projectile axis with respect to the unperturbed axis. This is illustrated in Fig. (1). The projectile is assumed to be rigid and symmetric with respect to the center of mass and is assumed to have no spin. The extension to spinning projectiles and two transverse dimensions will be briefly considered at the end of this section. The projectile displacement is given as a function of time and distance along the projectile by:

$$x(t;z') = x_0 + z'\sin\theta \quad \sim x_0 + z'\theta \tag{1}$$

where z' is the length along the projectile measured from the center. We assume that the transverse forces due to the coils are given per unit length by $f_c(t;z')$ and the flyway restoring force per unit length is given by: $f_r(t;z') = -kx(t;z')$. This later assumption needs to be modified according to the physical response of the flyway tube material. Modification of the above force to act only on a certain length of the projectile, for example the front or rear, results only in a change in the coefficients in the equations of motion. We can write the equation of motion for the center of mass by integrating over all the transverse forces and we get:

$$M_p \frac{d^2 x_o}{dt^2} = \int_{-l}^{l} dz' f_c(t;z') - 2klx_o(t) \tag{2}$$

where M_p is the total projectile mass and l is the half length. The equation for the rotation angle θ is more complex and can be derived by considering the projectile angular momentum. The angular momentum with respect to a fixed point (in the lab frame) located on the unperturbed axis is found to be:

$$\vec{L} = M_p \left(-x_o v_z + \frac{dx_o}{dt} z + \frac{l^2}{3}\frac{d\theta}{dt}\right) \hat{y} \tag{3}$$

where v_z is the axial speed and z is the distance of the projectile center of mass from the fixed reference point. The equation of motion is: $d\vec{L}/dt = \vec{\tau}$, where $\vec{\tau}$ is the applied torque. The resulting equation is:

$$M_p \left(-x_o \frac{dv_z}{dt} + z\frac{d^2 x_o}{dt^2} + \frac{l^2}{3}\frac{d^2\theta}{dt^2}\right) = \int_{-l}^{l} dz' (z'+z)(f_c + f_r) - \int d^3r' \tilde{x} F_z \tag{4}$$

where F_z is the axial force per unit volume on the projectile, $\tilde{x}$ is the moment arm given by: $\tilde{x} = x_o + z'\theta + r'\sin(\varphi')$, and the integral over d^3r' is over the projectile volume, that is $d^3r' = r'dr'd\varphi'dz'$ with r' and φ' measured with respect to the projectile axis. Since the axial equation of motion just gives the acceleration in terms of the total axial force, that is $M_p \frac{dv_z}{dt} = \int d^3r' F_z$, and d^2x_o/dt^2 is described by Eq. (2), Eq. (4) reduces to:

$$\frac{M_p}{3} l^2 \frac{d^2\theta}{dt^2} = \int_{-l}^{l} dz' z' \left[f_c(t;z') - \theta(t) f_z(t;z')\right] - \int d^3r' \left[r' \sin\varphi'\right] F_z - \frac{2}{3} l^3 k\theta(t) \tag{5}$$

where f_z is the axial force per unit length, that is F_z integrated over the projectile cross section. The first term on the RHS of Eq. (5) is torque due to coil transverse forces and can be either stabilizing or destabilizing. The second term is the torque due to the axial force and is stabilizing if the force is concentrated toward the front of the projectile and destabilizing if it is concentrated toward the rear. The third term is the torque due to asymmetry of the axial force in the azimuthal coordinate. This also can be either stabilizing or destabilizing. The fourth term is the restoring torque due to reaction of the flyway tube and is always stabilizing. Thus if the coil-projectile interactions are known, the above equations can be solved and the flyway tube displacement and stress profiles can be obtained.

For the case of a projectile with spin, all three dimensions have to be considered. If the projectile spins with an angular frequency ω, and the rotation angles along x and y are denoted by θ_x and θ_y, then for small rotation angles, the angular momentum vector is given by:

$$\vec{L} = I_0 \omega (\hat{z} + \theta_x \hat{x} + \theta_y \hat{y})$$

where I_0 is the moment of inertia given by: $I_0 = M_p R^2/2$. With the assumption of axi-symmetry (to zeroth order), the torque in the axial direction is zero and thus the axial component of $d\vec{L}/dt$ is zero, which implies that ω is constant in time. Thus we have: $\frac{d\vec{L}}{dt} = I_0 \omega (\frac{d\theta_x}{dt}\hat{x} + \frac{d\theta_y}{dt}\hat{y})$. The effect of these spin terms has to be compared with other terms in Eq. (5). For a fixed torque, and if ω is large, $d\theta/dt$ will be small and thus spin will have the effect of reducing rotational motion. We also note that since the spin term in the angular momentum equation is first order in $d\theta/dt$, it is a damping term. How much damping there is will depend on the relative magnitudes of the terms.

III. Coil-Projectile Interactions - Displaced Projectile Element

We first consider the transverse force and torque on a projectile element that results when it is displaced co-axially from a coil by a small amount. Using the fact that the magnetic flux at a projectile element due to coil current I_i is given by: $\Phi_{ij} = M_{ij} I_i$, where M_{ij} is the mutual inductance between the coil (denoted by i) and the projectile element (denoted by j), we find that the axial and radial magnetic fields can be written as:

$$B_z(r,z) = \frac{I_i}{2\pi r}\frac{\partial M_{ij}}{\partial r}, \text{ and } B_r(r,z) = \frac{-I_i}{2\pi r}\frac{\partial M_{ij}}{\partial z} \qquad (6)$$

Now if the projectile element is displaced a distance x, we can still write the axial field along the projectile element as:

$$B_z(\psi) = \frac{\tilde{I}_i}{2\pi\tilde{r}}\frac{\partial}{\partial r}M_{ij}(\tilde{r}) \;, \quad B_r(\psi) = -\frac{\tilde{I}_i}{2\pi\tilde{r}}\frac{\partial}{\partial z}M_{ij}(\tilde{r}) \tag{7}$$

where $\tilde{r}$ and ψ are the radius and angle measured from the unperturbed center (see Fig. (2)), and $\tilde{I}_i$ is the perturbed coil current. The net transverse force on the projectile element for small displacements can be written as:

$$F_x = \int_0^{2\pi} d\psi\,(r\sin\psi)\,\tilde{I}_j B_z(\psi)$$

$$= \frac{1}{2\pi}\int_0^{2\pi} d\psi \tilde{I}_i\tilde{I}_j \sin\psi\left(\frac{\partial M_{ij}}{\partial r} + \frac{\partial^2 M_{ij}}{\partial r^2}(\tilde{r}-r)\right) \tag{8}$$

Keeping lowest order terms in the displacement we find: $\tilde{r} = r + x\sin(\psi)$ and thus the transverse force to lowest order is given by:

$$F_x = \frac{I_i I_j}{2} x \frac{\partial^2 M_{ij}}{\partial r^2} \tag{9}$$

In writing Eq. (8) we have assumed that the current density of the projectile element under consideration remains uniform and the current is along the azimuthal direction only. This is true for projectiles that are thin compared to a skin depth or for litz type elements. For a solid projectile, the current flow pattern might become very complex as the projectile is displaced and fields are setup to maintain the magnetic field. To do this problem correctly a 3-D solution is required. However, the above analysis yields an upper limit on the transverse force for the solid projectile case. The reason for this assertion is the fact that for a perfectly conducting projectile, the magnetic field would be frozen implying that the current would also be frozen with respect to unperturbed space as the projectile is displaced. In this case the net transverse force would vanish. For finite resistivity we expect that the net transverse force will be somewhere between the perfectly conducting and uniform current density cases. The second derivative term of the mutual inductance in Eq. (9) can (+) or (-) depending on the details of the geometry. Thus the transverse force can be stabilizing or destabilizing. In general if $I_i I_j < 0$, and if the projectile element radius is smaller than the coil radius, this force is stabilizing for small axial separation and destabilizing for large axial separations. As a numerical example we consider coil parameters (navy gun): $R_i = 0.105$, $R_o = 0.155$, $z_1 = 0.0$ and $z_2 = 0.05$ meters with 20 turns and projectile element parameters: $R_i = 0.09$, $R_o = 0.10$, $z_1 = 0.05$ and $z_2 = 0.06$ meters, we find (using Slingshot

inductance calculation): $M_{ij} = 2.9\times10^{-6}$ H, $\frac{\partial M_{ij}}{\partial r} = 6.8\times10^{-5}$ H/m and $\frac{\partial^2 M_{ij}}{\partial r^2} = 7.8\times10^{-4}$ H/m^2.

Thus the ratio between the transverse force (for $x = 3\times10^{-4}$ m) and the total radial force (given by: $F_r = I_i I_j \partial M_{ij}/\partial r$) for these elements is: $F_x/F_r = 1.7\times10^{-3}$. This is a relatively small force but is not insignificant. This example gives a rough estimate of the transverse force between a coil and a projectile element. Since the second radial derivative of the mutual inductance can vary significantly with axial separation, the transverse force is also a strong function of the axial separation.

In addition to the transverse force, there is a net torque due to the distribution of the axial force in the azimuthal direction, which is given by the third term on the RHS of Eq. (5). Using the expression for the radial magnetic field given by Eq. (6), we find the axial force distribution along the projectile element for small displacements is given by:

$$F_z(\psi) = -I_j B_r(\psi)$$

$$= \frac{I_i I_j}{2\pi\tilde{r}}\left(\frac{\partial M_{ij}}{\partial z} + \frac{\partial^2 M_{ij}}{\partial z \partial r}(\tilde{r} - r)\right),$$

where J_j is the current density of the projectile element. This equation assumes that the cross section of the element is small enough so that there is no significant field variation across it. Multiplying by the moment arm, with respect to projectile axis ($r' \sin(\varphi')$), and integrating over the volume and keeping lowest order terms in displacement we find (see Fig. (2)):

$$\int d^3r' \left[r' \sin\varphi'\right] F_z(\psi) = \frac{I_i I_j}{2} r x \frac{\partial^2 M_{ij}}{\partial r \partial z}, \tag{10}$$

where r is the projectile element radius and x is the displacement. Equations (9) and (10) can now be summed over coil and projectile elements and used in the equations of motion.

IV. Coil-Projectile Interactions - Tilted Projectile Element

If the projectile element axis is tilted at an angle μ with respect to the unperturbed axis, we can write the magnetic field due to the coil along the projectile element azimuth as:

$$B_z(\psi) = \frac{1}{2\pi r} I_i \left(\frac{\partial M_{ij}}{\partial r} - \frac{\partial^2 M_{ij}}{\partial r \partial z}(r\mu \sin\psi)\right) \tag{11}$$

and

$$B_r(\psi) = \frac{-1}{2\pi r} I_i \left(\frac{\partial M_{ij}}{\partial z} - \frac{\partial^2 M_{ij}}{\partial z^2} (r\mu \sin\psi) \right) \tag{12}$$

In Eqs. (11-12) we have assumed that $\mu \ll 1$ and kept only lowest order terms. Carrying out the proper integrals over the projectile element azimuth, the lowest order transverse force is:

$$F_x = I_j \int_0^{2\pi} d\psi r B_z(\psi) \sin(\psi) = -\frac{I_i I_j}{2} \mu r \frac{\partial^2 M_{ij}}{\partial r \partial z} \tag{13}$$

The axial force per unit volume along the projectile element is $F_z(\psi) = -I_j B_r(\psi)$ and the resulting torque is (third term on RHS of Eq. (5)):

$$\int d^3r' \, |r' \sin\varphi'| \, F_z(\psi) = -I_j \int_0^{2\pi} d\psi r B_r(\psi) \, |r \sin\psi|$$

$$= -\frac{I_i I_j}{2} \mu r^2 \frac{\partial^2 M_{ij}}{\partial z^2} \tag{14}$$

Equations (13) and (14) are the required terms in the angular momentum equation. Also note that the sign of the torque is already taken care of in Eq. (5). Another term that is not accounted for in the angular momentum equation is the torque due to the zeroth order radial force, $F_x(\psi) = I_j B_z(\psi) \sin\psi$, combined with a tilt. This torque results from the radial force acting with a moment arm of magnitude $-r\mu \sin\psi$ and is given by:

$$\tau_y = -I_j \int_0^{2\pi} d\psi r B_z(\psi) \sin\psi \, |r\mu \sin\psi|$$

$$= -\frac{I_i I_j}{2} \mu r \frac{\partial M_{ij}}{\partial r} \tag{15}$$

Equations (13), (14) and (15) are the force and torque on a tilted projectile element due to an unperturbed coil. If the coil is tilted by an angle μ, the projectile-coil system can be rotated by an angle $(-\mu)$ and is thus equivalent to an unperturbed coil and a projectile element that is tilted by an angle $(-\mu)$ and displaced by an amount $Z_{ij}\sin(-\mu)$, where Z_{ij} is the axial separation between coil and projectile element. Since only small displacements and tilts are considered (only first order terms are kept), the resulting transverse force and torque add linearly for a combined tilt and displacement.

V. Analysis of Projectile Stability for a Multi-Coil Launcher

In a real electromagnetic launcher the projectile is made up of many elements, each of which is acted upon by several coils. Since the projectile is assumed rigid, projectile-projectile interactions need not be considered. We assume that each coil has a tilt μ_i and displacement x_i. Thus the effective tilt for each projectile element is $(\theta-\mu_i)$ and the effective displacement is $(x_o+\theta z_j - Z_{ij}\mu_i - x_i)$, where z_j is the element's axial position with respect to the projectile center of mass and Z_{ij} is the distance between centers of coil and element. Using the above expressions for transverse force and torque due to displacement and tilt and summing over coils and projectile elements (replace integrals over dz' by summation over projectile elements), the equations of motion become:

$$M_p \frac{d^2 x_o}{dt^2} = \sum_{ij} \frac{I_i I_j}{2} \Lambda_{ij} - 2klx_o(t) \tag{16}$$

and

$$\frac{M_p}{3} l^2 \frac{d^2\theta}{dt^2} = \sum_{ij} \frac{I_i I_j}{2} \left(z_j \Lambda_{ij} - 2\theta(t) z_j \frac{\partial M_{ij}}{\partial z} - (\theta-\mu_i) r_j \frac{\partial M_{ij}}{\partial r} - \Gamma_{ij}\right) - \frac{2}{3} l^3 k\theta(t) \tag{17}$$

where Λ_{ij} and Γ_{ij} are given by:

$$\Lambda_{ij} = \left((x_o + z_j\theta - x_i - Z_{ij}\mu_i) \frac{\partial^2 M_{ij}}{\partial r^2} - r_j (\theta-\mu_i) \frac{\partial^2 M_{ij}}{\partial r \partial z} \right)$$

and

$$\Gamma_{ij} = \left(r_j (x_o + z_j\theta - x_i - Z_{ij}\mu_i) \frac{\partial^2 M_{ij}}{\partial r \partial z} - r_j^2 (\theta-\mu_i) \frac{\partial^2 M_{ij}}{\partial z^2} \right)$$

The sum over i is over all coils and sum over j is over all projectile elements. Equations (16) and (17) can be easily incorporated in the Slingshot code and for a given coil displacement and tilt profiles these equations can be solved to yield the projectile displacement and rotation as a function of time. This can then be used to determine the stresses on the flyway tube.

Both coil displacement and tilt lead to projectile displacement and rotation of similar magnitudes. Thus without loss of generality we restrict ourselves to the case with only coil displacement. Since the equations of motion need to be solved for x_0 and θ as functions of time, it is useful to isolate these variables in Eqs. (15) and (16). Doing this, and assuming all the μ_i's are zero, these equations can be written in the form:

$$\frac{d^2x_0}{dt^2} = Ax_0 + B\theta + C \tag{18}$$

$$\frac{d^2\theta}{dt^2} = \alpha x_0 + \beta\theta + \gamma \tag{19}$$

where the coefficients are functions of time and are given by:

$$A = \frac{1}{M_p}\left[\left(\sum_{ij}\frac{I_iI_j}{2}\frac{\partial^2 M_{ij}}{\partial r^2}\right) - 2kl\right]$$

$$B = \frac{1}{M_p}\sum_{ij}\left(\frac{I_iI_j}{2}\right)\left(z_j\frac{\partial^2 M_{ij}}{\partial r^2} - r_j\frac{\partial^2 M_{ij}}{\partial r\partial z}\right)$$

$$C = \frac{-1}{M_p}\sum_{ij}\frac{I_iI_j}{2}x_i\frac{\partial^2 M_{ij}}{\partial r^2}$$

$$\alpha = 3\frac{B}{l^2}$$

$$\beta = \frac{3}{l^2M_p}\left[\sum_{ij}\left(\frac{I_iI_j}{2}\right)\left(z_j^2\frac{\partial^2 M_{ij}}{\partial r^2} - 2z_jr_j\frac{\partial^2 M_{ij}}{\partial r\partial z} + r_j^2\frac{\partial^2 M_{ij}}{\partial z^2} - 2z_j\frac{\partial M_{ij}}{\partial z} - r_j\frac{\partial M_{ij}}{\partial r}\right) - \frac{2}{3}kl^3\right]$$

$$\gamma = -\frac{3}{l^2 M_p}\sum_{ij}\left(\frac{I_i I_j}{2}\right)\left(z_j\frac{\partial^2 M_{ij}}{\partial r^2} - r_j\frac{\partial^2 M_{ij}}{\partial r \partial z}\right)x_i$$

The terms C and γ are the forcing terms and they are proportional to the displacement of the coils. Since we only considered first order terms in displacement and rotation the equations of motion are linear and thus are only valid for small perturbations.

Even though all the terms in the coefficients of Eqs. (18) and (19) have strong time dependence, we expect that these coefficients represented by the sums over coils and projectile elements are only slowly varying in time similar to the axial acceleration. Of course we expect very fast oscillations in these coefficients similar to those in the axial acceleration due to the discreteness of the coils and fast rise time, but the amplitude of these oscillations is small and the projectile transverse motion is not expected to respond to these oscillations. Another slow time variation of the coefficients is expected because of finite slip speeds. Because of the slow time variation (over many coils) we can approximate these coefficients by constants and get a reasonably good idea about the resonant frequencies of the launcher. These resonant frequencies are found from the roots of the characteristic equation which is obtained by assuming solutions of the form $e^{i\omega t}$ in the homogeneous equations of motion, that is roots of the equations:

$$-\omega^2 x_0 - A x_0 - B\theta = 0$$

$$-\omega^2\theta - \alpha x_0 - \beta\theta = 0$$

or:

$$(\omega^2 + A)(\omega^2 + \beta) - \alpha B = 0$$

with solutions:

$$\omega^2 = \frac{-(A+\beta) \pm \sqrt{(A-\beta)^2 + 4\alpha B}}{2} \qquad (20)$$

Equation (20) shows that there is the possibility of unstable solutions, depending on the values of the coefficients. If A and β are negative and $|A+\beta| > \sqrt{(A-\beta)^2 + 4\alpha B}$ then all solutions are stable, otherwise projectile transverse motion is unstable. We note that for all values of the coefficients, there exists a value of the flyway restoring force constant k that would make $A+\beta$ large enough negative to stabilize the motion.

For a stable projectile, there are two frequencies given by Eq. (20) at which the projectile can naturally oscillate. If the coils are displaced at a certain axial wavelength λ, the forcing terms given by C and γ in Eqs. (18,19) will have a time dependence roughly of the form $e^{i\omega_0 t}$, where $\omega_0 = (2\pi v_z)/\lambda$, and v_z is the projectile axial speed. If ω_0 matches one of the natural frequencies, a resonance condition will develop which will result in a secularly growing oscillation amplitude. However, since v_z is a changing function of time, this resonance condition will not be maintained. After the resonance, the projectile will continue to oscillate at its natural frequencies with a contribution due to the forcing term. Physically it is expected that coil displacement will be randomly distributed axially in the launcher. In such a case growth of the displacement amplitude due to resonance will depend on the distribution of wavelengths in the displacement profiles.

VI. Numerical Solution and Results

As mentioned previously, the complexity of the coefficients of the equations of motion necessitates a numerical solution in order to obtain quantitative information about stability and displacement growth. Implementation of such a numerical solution is straightforward in the Slingshot code. Slingshot is a 2-D simulation code that represents electromagnetic interactions between coils and projectile elements by a circuit model. The circuit equations solved are very similar to those in the WARP-10 code described in Ref. (3). In Slingshot the mutual inductances and their radial and axial derivatives are calculated analytically for circular loops of rectangular cross section using Lyle's method. The second order derivative terms in the coefficients of Eqs. (18,19) are evaluated numerically using the Slingshot values of the first derivatives. The equations of motion are then integrated using the normal Slingshot time step in a leap-frog algorithm.

Several simulations were run for the 20 meter navy gun parameters, with a solid aluminum armature. The parameters used are as follows:

Projectile: $r_i = 0.055$ m, $r_o = 0.095$ m, $L = 2l = 0.4$ m

Coils (270 stages): $r_i = .105$ m, $r_o = 0.185$ m, thickness = 0.06, fill factor = 0.2
gap = 0.015 m.

Capacitors: C = 1600 μF

Voltage: 5 @ 20 kV, 5 @ 24 kV, 5 @ 28 kV, 5 @ 32 kV, 5 @ 35 kV, 5 @ 37 kV,
240 @ 40 kV (1.2 MJ/stage)

Circuit Parameters: $R_a = 1$ mΩ, $R_b = 25$ mΩ, $R_c = 1$ mΩ,
$L_a = 0.1$ μH, $L_b = 2.5$ μH, $L_c = 0.1$ μH

Initial coil and projectile temperature = 20 C

Total projectile mass = 60 kg

Initial speed = 10 m/sec

Proportional slip is used with $\alpha = 12x10^{-3}$

Rise length = 0.18 m

Number of turns: Determined by the code based on a fixed rise length.

For these parameters the final velocity is V_f = 1791 m/sec. The grading of the coil energy for the first 30 stages is for the purpose of controlling the temperature rise.[6] For the above parameters, the value of the flyway spring constant for which the displacement solution is stable is $k \approx 1.0x10^8$ N/m^2. This is also the value for which $\omega_2^2(t)$ is non-negative for all time.

We performed three simulations with $k = 1.5x10^8$ N/m^2 and using the following coil displacement profiles:

$$(1\text{-}2) \qquad x_i = A_o \sin\left(\frac{2\pi z_i}{\lambda}\right)$$

$$(3) \qquad x_i = 2A_o[0.5 - R]$$

where z_i and x_i are the axial location and displacement of the ith coil respectively and R is a random number (between 0.0 and 1.0). In Fig. (3) the projectile axial history is shown and in Fig. (4) the coefficients of the equations of motion A,B, α, and β and the resulting natural frequencies ω_1 and ω_2 are shown. These coefficients and frequencies are independent of the coil displacement profile. The external force coefficients C and γ along with the displacement and rotation are shown vs. projectile axial position in Figs. (5-7) for three coil displacement profiles. In these figures we also show plots of the displacement and rotation vs. time. As expected, the forcing terms C and γ show the nature of the coil displacements at the imposed wavelengths with a time dependent amplitude. Although the coefficients vary with time, the basic mechanism for growth of the transverse displacement and rotation is as discussed in the previous section, namely due to resonant interaction with the driving forces. The case with random coil displacement also shows significant amplitudes, but slightly less than the other two cases. The reason for this growth is the existence of long wavelengths components in the driving forces as can be readily seen in the plots of C and γ. For a more detailed description of the distribution of wavelengths, an FFT could be applied.

In the figures, the transverse oscillations continue after the projectile leaves the launcher (20 meters). This is because the flyway restoring forces are not turned off in the simulations after the projectile leaves. After the projectile leaves, all the coil forces go to zero and the limit of the natural frequency becomes: $\omega_1 = \omega_2 = \sqrt{kl/M_p}$. This causes the observed increase in wavelength and amplitude.

For a coil displacement of 1 mm, the transverse oscillation amplitude is approximately 4mm for a flyway constant of 1.5×10^8 N/m^2. In this case the transverse force per unit length exerted by the flyway tube is: $F_r = kx_o = 6 \times 10^5$ N/m. If this force is distributed over a fraction μ of the circumference, the pressure is: $P = F_r / (2\pi R\mu) \approx 50$ bars, which is reasonable. For a more accurate estimate of the transverse pressure, the restoring force law needs to be modified to account for the detailed structures used in the launcher. The projectile transverse velocity at the muzzle is roughly 5 m/sec, which is less than 0.3% of the axial velocity. The rotation frequency at the muzzle ($d\theta/dt$) is roughly 3 Hz, which can be easily spin stabilized.

VI. Summary of Results

The equations of motion for both translation and rotation of a projectile in an electromagnetic induction launcher were derived. The electromagnetic interactions between coils and displaced or tilted projectile elements were calculated based on a first order perturbation method, assuming that the perturbed current flows in an azimuthally symmetric fashion with respect to the displaced projectile element. To account for the breaking of this symmetry a 3-D model is required in which fields and currents would have to be calculated at all points in the projectile. The usefulness of the present model is the fact that it provides an upper limit estimate of the transverse forces and displacements and the relative ease of incorporating it in the 2-D Slingshot code.

Depending on the parameters, the transverse motion can be unstable. However, by increasing the spring constant for the flyway tube the motion can be stabilized in those situations. For the 20 meter navy gun parameters, and restoring force per unit length proportional to the local displacement, the value of the spring constant for which stable motion occurs is $k \approx 1.0 \times 10^8$ N/m^2. Numerical simulations were performed for the 20 meter navy gun parameters with $k = 1.5 \times 10^8$ N/m^2 and the resulting displacements are of the order of 4 mm, for coil displacements of 1 mm amplitude. For these values, a rough estimate of the transverse pressure on the flyway tube is about 50 bars. The growth in amplitude is due to a resonant interaction between projectile and the coil displacement profile. This resonant interaction does not persist because of the rapidly changing axial velocity. The higher the axial velocity, the longer the wavelength required for resonance.

The restoring force law used in the above analysis is highly idealized and is certainly not adequate to describe the complex structure of a launcher. An accurate description of the restoring force law is needed in which both axial and transverse dependences are prescribed. Such a prescription can be easily implemented in the numerical solution.

References

1. M. Cowan, M. M. Widner, E. C. Cnare, B. W. Duggin, R. J. Kaye and J. R. Freeman, "Exploratory Development of the Reconnection Launcher 1986-1990," IEEE Transactions on Magnetics, Vol. 27, No. 1, January 1991.

2. R. J. Kaye, E. L. Brawley, B. W. Duggin, E. C. Cnare, D. C. Rovang and M. W. Widner, "Design and Performance of a Multi-Stage Cylindrical Reconnection Launcher," IEEE Transactions on Magnetics, Vol. 27, No. 1, January 1991.

3. M. M. Widner, "WARP-10: A Numerical Simulation Model for the Cylindrical Reconnection launcher," IEEE Transactions on Magnetics, Vol. 27, No. 1, January 1991.

4. M. Cowan and I. R. Shokair, "Advantages of a Wound Armature," Sandia Internal memo, March 15, 1993.

5. B. M. Marder, Private Communication.

6. I. R. Shokair and M. Cowan, "Summary of Navy Gun Simulations," Sandia Internal memo April 20, 1993.

Acknowledgments

The author would like to thank M. Cowan, R. Kaye, and B. Marder for useful discussions and comments. This work was supported by the Department of Energy under Contract No. DE-AC04-76DP00789.

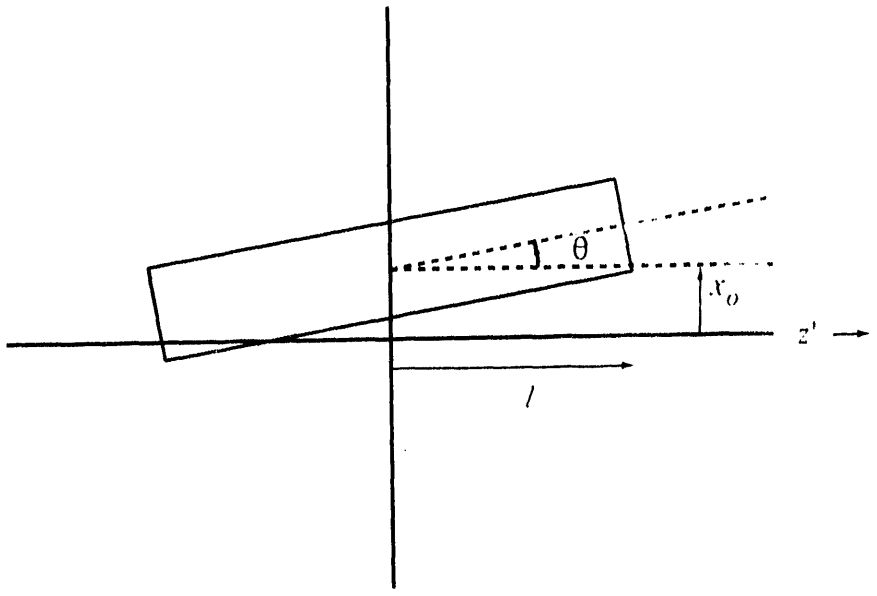

Fig. 1. Geometry of displaced projectile

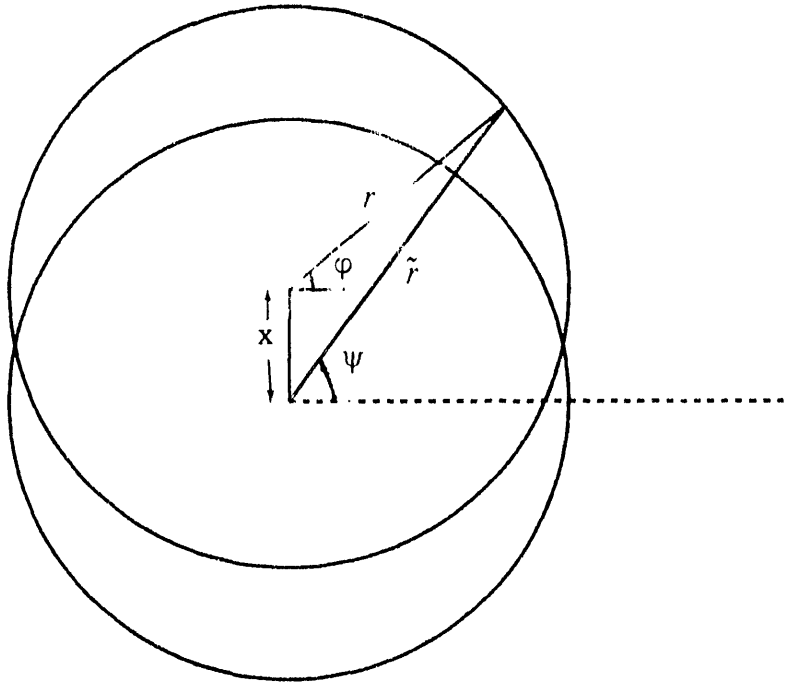

Fig. 2. Cross section of displaced projectile

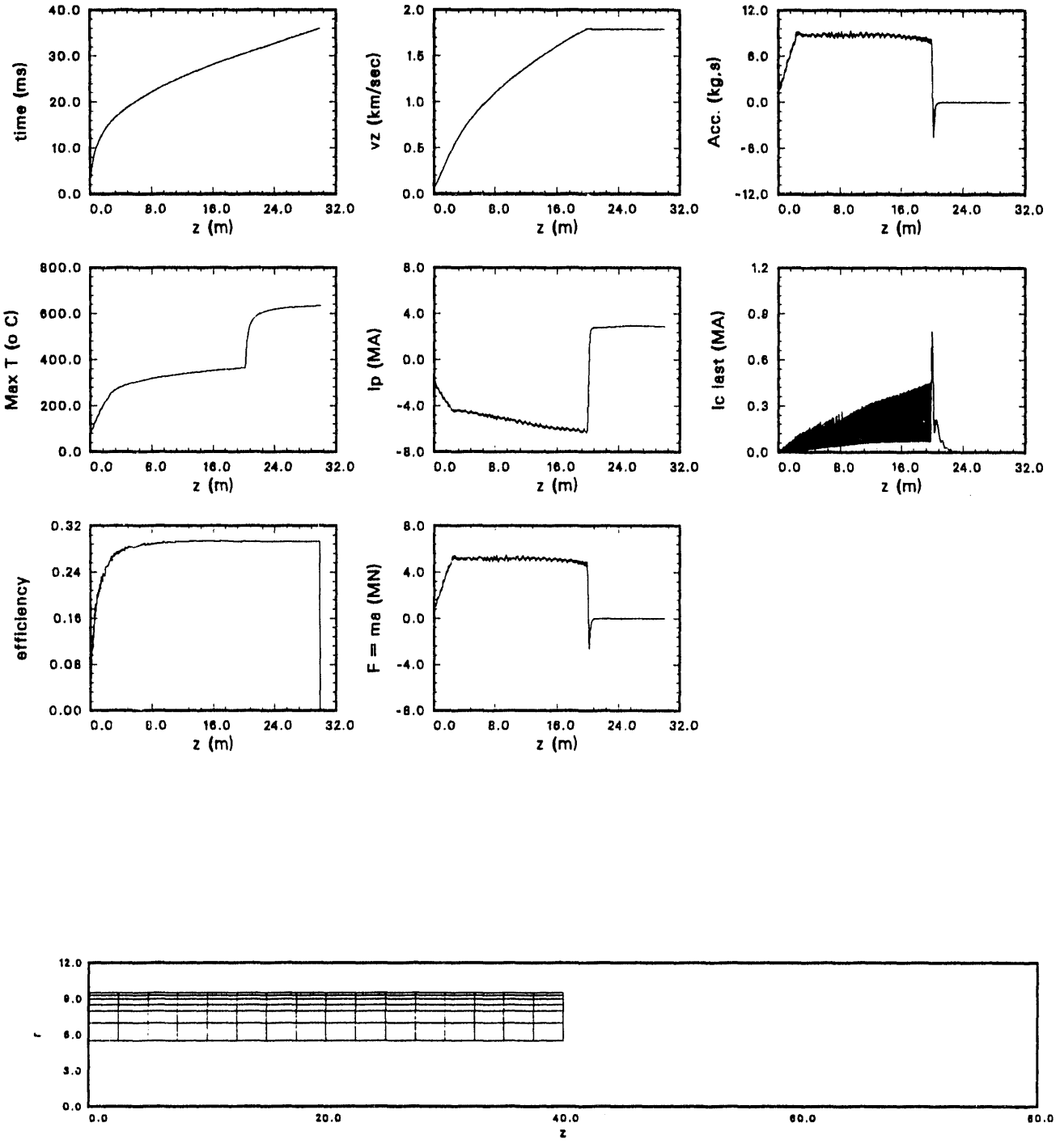

Fig. 3. Axial history of projectile for 20 meter navy launcher

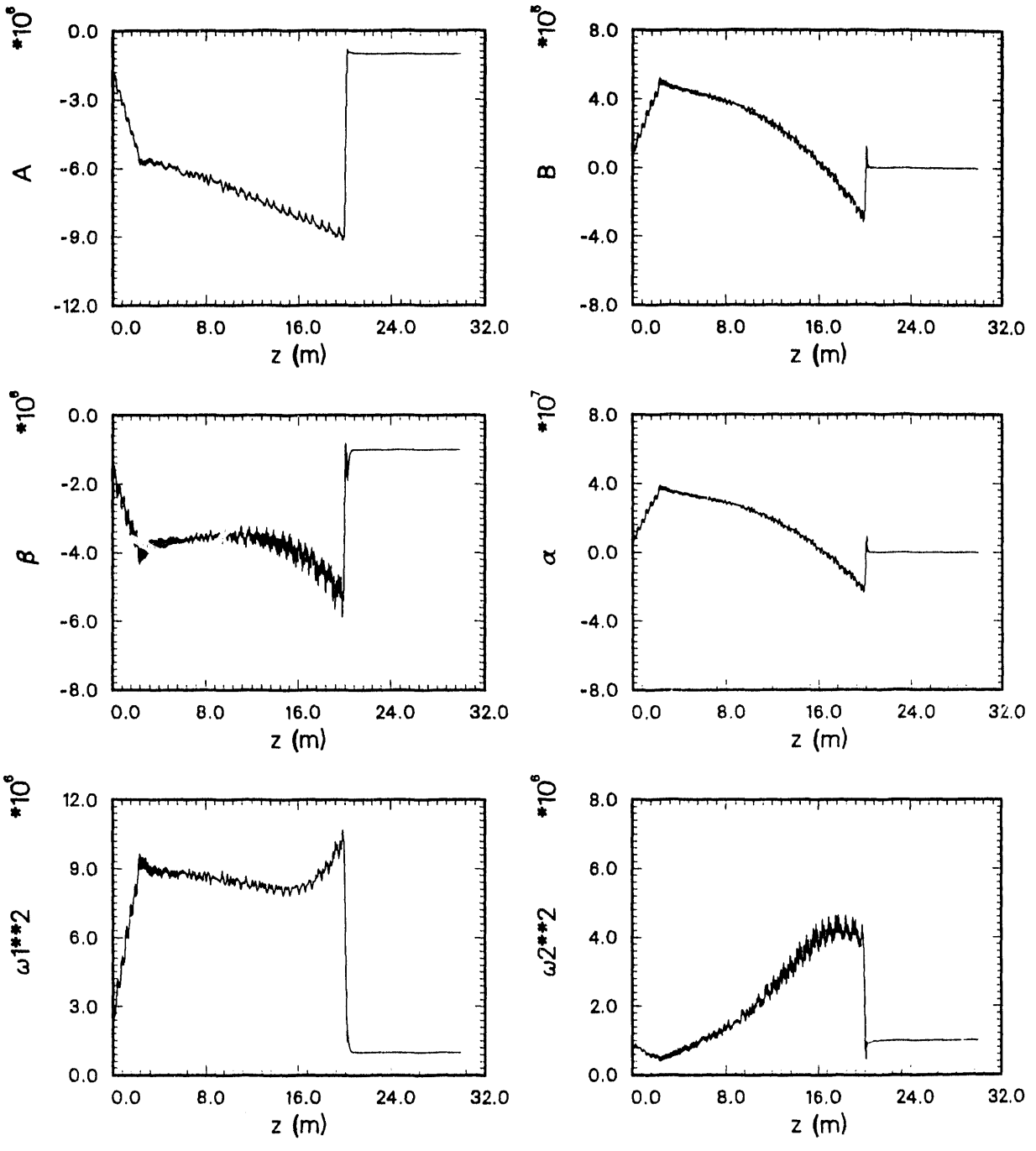

Fig. 4. Coefficients of the equations of motion and natural frequencies for the 20 meter navy gun parameters.

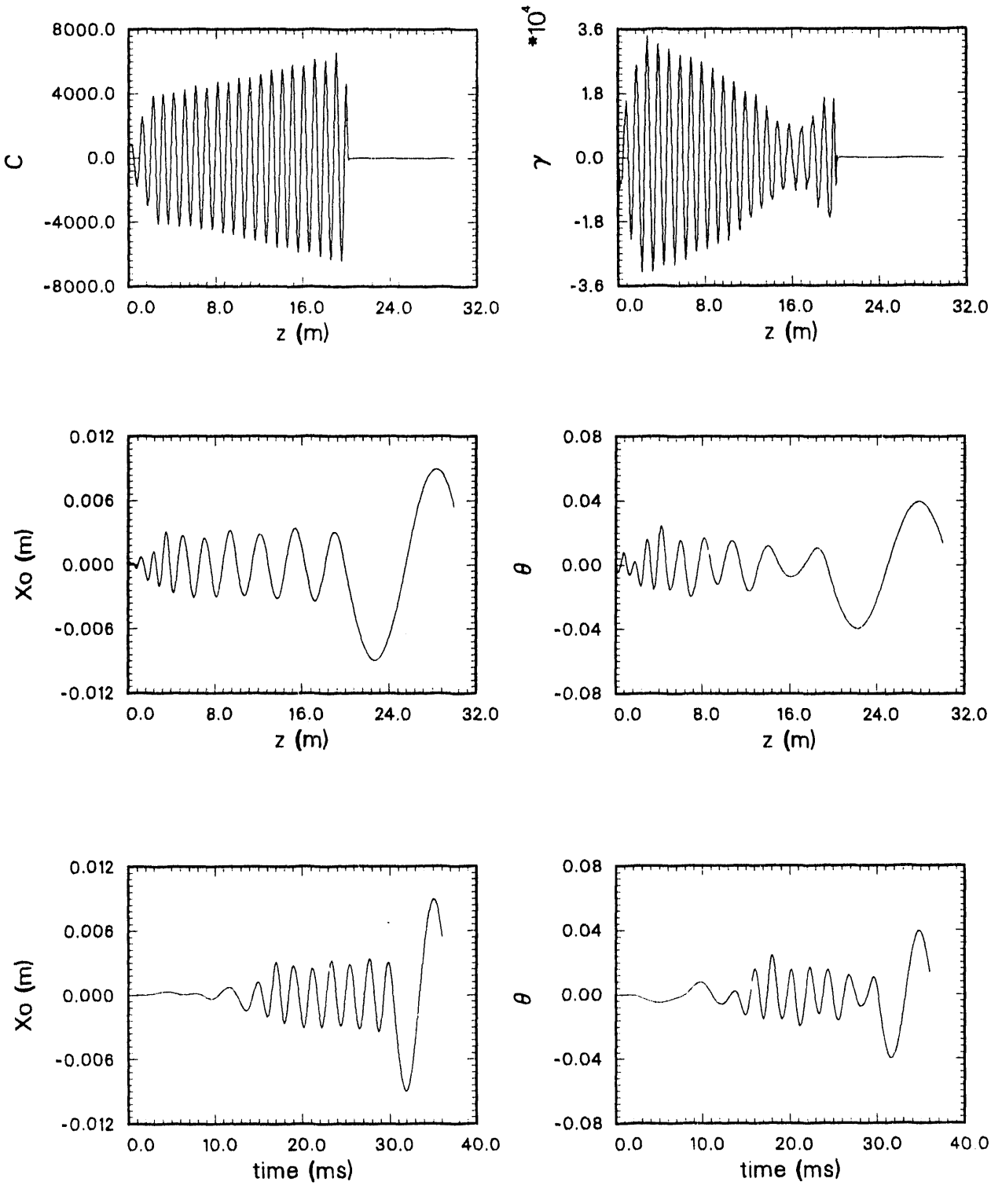

Fig. 5. Transverse motion for coil displacement of the form: $x_i = A_o \sin\left(\frac{2\pi z_i}{\lambda}\right)$, for A_0 = 1 mm and λ = 1 meter

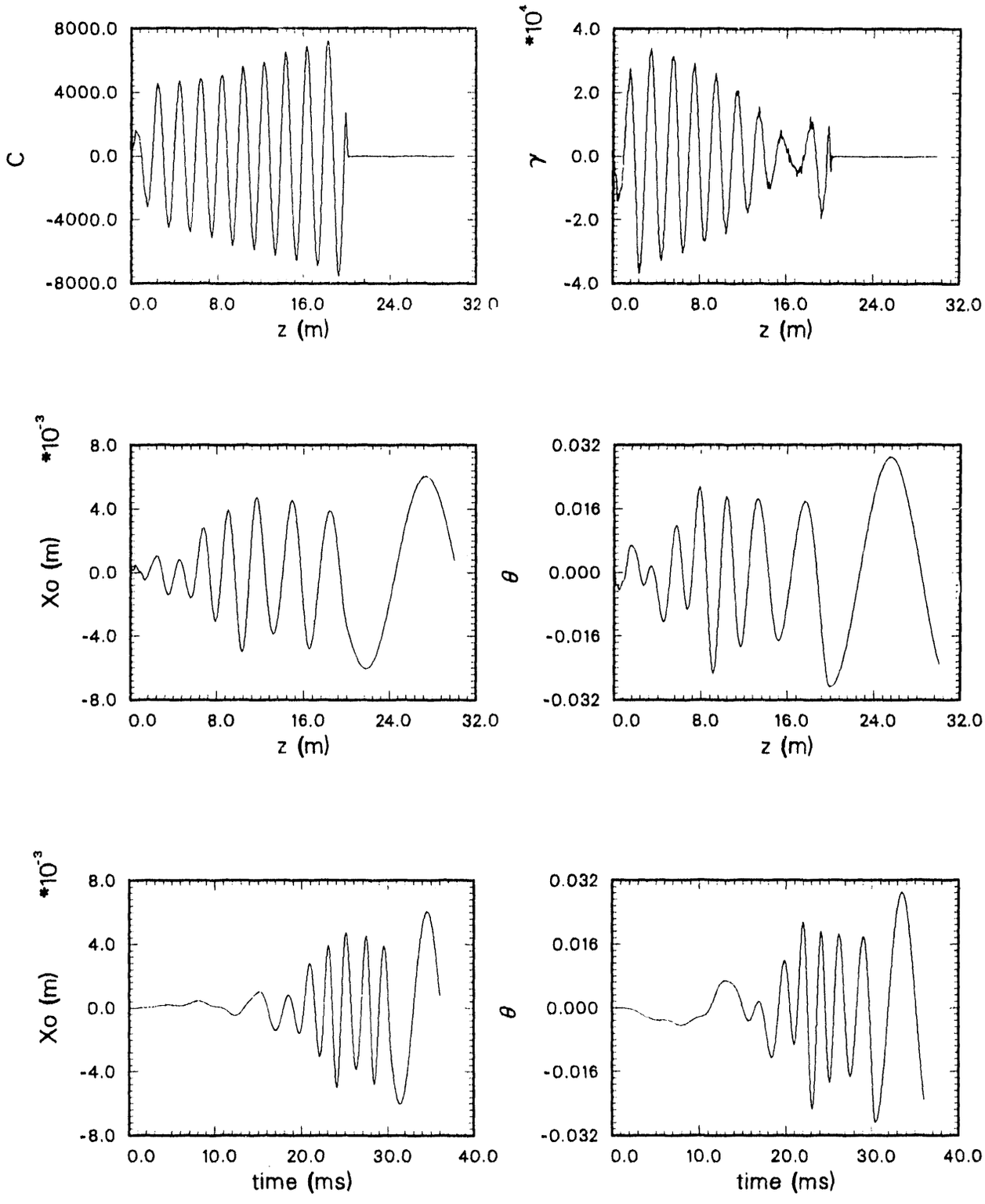

Fig. 6. Transverse motion for coil displacement of the form: $x_i = A_o \sin\left(\frac{2\pi z_i}{\lambda}\right)$, for A_o = 1 mm and λ = 2 meters

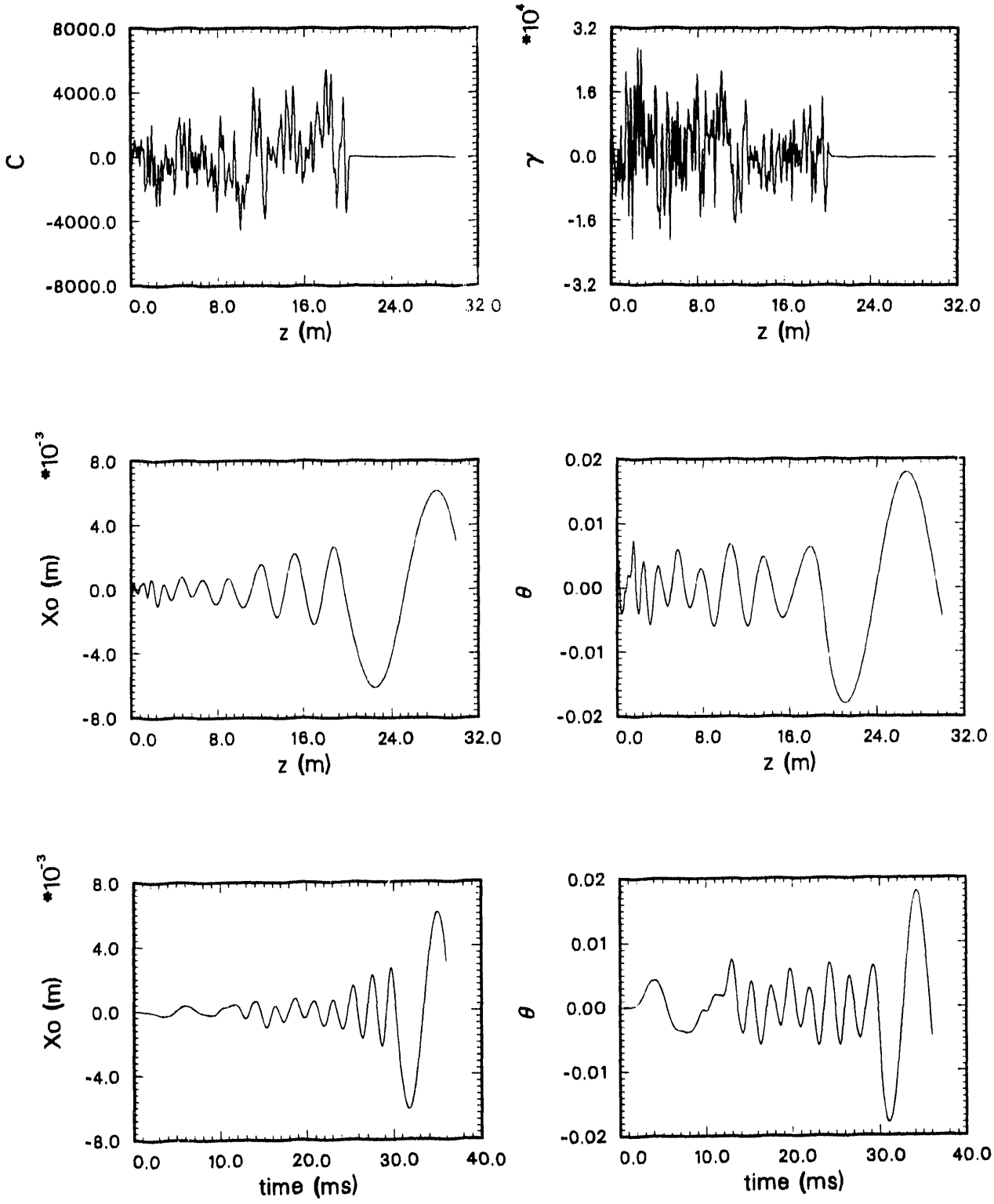

Fig. 7. Transverse motion for coil displacement of the form: $x_i = 2A_o[0.5 - R]$ for A_o = 1 mm and R is a random number between 0 and 1.

DISTRIBUTION:
Unlimited Release

Dwight Dustin
SMDO/IST
Pentagon
Washington, DC 20301-7100

Leonard H. Caveny
SMDO/IST
Pentagon
Washington, DC 20301-7100

Maj. Michael Huebschman
SMDO/IST
Pentagon
Washington, DC 20301-7100

Michael D. Griffin
NASA Headquarters
Mail Code X
1225 Jefferson Davis Hwy., Suite 1300
Alexandria, VA 22202

Norman W. Lee, Jr.
ANSER, Suite 800
1215 Jefferson Davis Hwy.
Arlington, VA 22202

Lt. Col. Roger Lenard
Phillips Lab/XPM
Kirtland AFB, NM 87117-6008

Miles R. Palmer
SAIC
1700 Goodridge Drive
McLean, VA 22102

John Hunter
University of California
LLNL
L-465
P. O. Box 808
Livermore, CA 94550

Commander
Naval Sea Systems Command (NAVSEA)
Attn: SEA-62y2 (Cdr. Allen R. Boutz)
Washington, DC 20362-5101

Commander
Naval Sea Systems Command (NAVSEA)
Attn: 06KR12 (Cdr. Craig Dampier)
Washington, DC 20362-5101

Center for Naval Analyses (CNA)
4401 Ford Avenue
Alcxandria, VA 22302-0286
Attn: Alan Berman
Vic Dawson
Robert Sullivan

A. J. Wittle
Martin Marietta
Aero & Naval Systems
103 Chesapeake Park Plaza
Mail Stop 522
Baltimore, MD 21220

Michael B. Hughes
Martin Marietta
Vice President, Business Development
Aero & Naval Systems
103 Chesapeake Park Plaza
Baltimore, MD 21220

Melvin M. Widner
General Dynamics
Land Systems Division
Mail Zone 436-21-14
P. O. Box 2074
Warren, MI 48090-2074

Hildi S. Naber-Libby
ARDEC
SMCAR-FSC
Bldg. 329
Picatinny Arsenal, NJ 07806-5000

Jerald Parker
Los Alamos National Laboratory
E526
P. O. Box 1663
Los Alamos, NM 87545

Richard McKenzie
Geodynamics Corp.
National Test Bed Program
Mail Stop N8930
Falcon AFB, CO 80912-5000

Brendan Godfrey
Phillips Lab/WS
Kirtland AFB, NM 87117-6008

W. James Sarjeant
University at Buffalo
Department of Electrical and
Computer Engineering
Bonner Hall (Rm. 312)
Buffalo, NY 14260

Alan J. Toepfer
SAIC
2109 Air Park Road, SE
Albuquerque, NM 87106

Internal Distribution:

1000	P. A. Fleury
1200	D. L. Cook
1203	K. R. Prestwich
1204	J. J. Ramirez
1221	B. N. Turman (5)
1221	E. C. Cnare
1221	M. Cowan
1221	R. J. Kaye
1239	F. J. Dempsey
1239	G. M. Douglas
1239	K. J. Shimp
1239	R. W. Wavrik
1241	C. L. Olson
1241	B. M. Marder
1241	I. R. Shokair (10)
4700	J. P. VanDevender
6514	R. J. Lipinski
9722	R. L. Woodfin
8523-2	Central Technical Files
7141	Technical Library (5)
7151	Technical Publications
7613-2	Document Processing for DOE/OSTI(10)

DATE
FILMED
12/13/93
END